Physics of Wave Processes and Radio Systems
2023, vol. 26, no. 1, pp. 9–17

DOI 10.18469/1810-3189.2023.26.1.9-17

Received 24 November 2022
Accepted 26 December 2022

Influence of nanoparticle dispersion in a transparent liquid on the spatial characteristics of a four-wave radiation converter

Valery V. Ivakhnik, Maxim V. Savelyev

Samara National Research University
34, Moskovskoye shosse,
Samara, 443086, Russian Federation

Abstract – The spatial characteristics of a four-wave radiation converter in a transparent heterogeneous polydisperse medium are studied in this paper considering the nanoparticle flow caused by the gravity action with a normal size distribution of particle. Three ranges of average nanoparticle radii (small, intermediate and large), for which different types of spatial spectra of the object waves are characteristic, are distinguished. Shown that in the range of small average nanoparticle radii an increase in the standard deviation leads to an increase in the half-width of the spatial frequency band cut out by a four-wave radiation converter from the spatial spectrum of the object wave. In the range of intermediate average nanoparticle radii an increase in the standard deviation can lead to both an increase and a decrease in the width of the «ring» cut out by a four-wave radiation converter. At large average nanoparticle radii a change in the standard deviation doesn't affect the spatial selectivity of the four-wave radiation converter.

Keywords – four-wave radiation converter; transparent medium; normal distribution.

Introduction

Interest in four-wavelength radiation converters (FRCs) is associated with the possibility of their use in solving many fundamental and applied problems, from transmitting information through optical waveguides and real-time image processing to creating single-photon sources for quantum computers and visualizing nanosized objects, including components of living cells and particles of noble metals [1–8]. In all of these problems, the accuracy of the FRC reconstruction of the wavefront of the wave incident on it, i.e., the correspondence between the spatiotemporal structures of the incident (signal) and reflected (object) waves, plays an important role.

FRC can be implemented in various nonlinear media, particularly heterogeneous media (e.g., suspensions and colloidal solutions), which have a nonresonant nonlinearity mechanism because of the creation of concentration and temperature gradients [9]. In heterogeneous media, high values of the nonlinear refractive index n_2 are achievable, which enables the use of low-intensity laser radiation when creating FRC [10; 11].

If we take a colloidal solution of nanoparticles as a nonlinear medium, then the energy of particles in the Earth's gravitational field is comparable to the energy of the thermal motion of liquid molecules [12; 13]. Therefore, when considering FRC implemented in such media, along with diffusion and electrostriction flows, the additional flow of nanoparticles caused by the action of gravity on them needs to be analyzed.

In Refs. [14–19], in the approximation of a small conversion coefficient, the spatial and temporal characteristics of FRC in a monodisperse transparent heterogeneous medium were investigated. The influence of interaction geometry, angular and frequency shifts, divergence of pump waves, absorption of the medium, and gravity flow on the spatial selectivity of FRC was analyzed.

In real heterogeneous media, the size distribution of nanoparticles [4; 20–23] affects both the temporal [24] and spatial characteristics of FRC. In this regard, this study examines the spatial selectivity of FRC in a transparent polydisperse heterogeneous medium, considering the flow of nanoparticles caused by the action of gravity on them.

1. Spatial spectrum of an object wave considering the force of gravity acting on nanoparticles of the same size in a transparent liquid

Let us consider the stationary mode of FRC operation in a transparent liquid with nanoparticles dissolved in it in a scheme with counterpropagating pump waves [17]. Two plane pump waves are incident on a horizontal layer of the medium located between the planes $z = 0$ and $z = 1$, propagating parallel to the Z-axis toward each other, with amplitudes A_1 and A_2

ivakhnik@ssau.ru (*Valery V. Ivakhnik*)

and a signal wave with amplitude A_3. Because of a degenerate four-wave interaction, an object wave with amplitude A_4 appears, propagating toward the signal wave, with a wavefront facing the signal wavefront.

In the approximation of a given field over pump waves and a small conversion factor, the intensity of radiation propagating in a nonlinear medium can be represented by the sum of the intensities of the pump waves and the terms because of the interference of the first pump wave and the signal wave. The spatial heterogeneity of radiation intensity as a result of diffusion, electrostriction, and the effect of gravity on nanoparticles leads to a spatial change in the concentration of nanoparticles. Because of the Dufour effect, a spatial change in the medium temperature δT also occurs. At particle concentrations less than 10^{12} cm^{-3} [4; 25], the change in the refractive index is determined mainly by the change in temperature, as follows:

$$n \approx n_l + \frac{\mathrm{d}n}{\mathrm{d}T}\delta T, \qquad (1)$$

where n_1 is the refractive index in the absence of radiation and (dn/dT) is the thermo-optical coefficient.

In Ref. [17], for a heterogeneous monodisperse nonlinear medium consisting of a transparent liquid and nanoparticles, under the condition of quasi-collinear propagation of interacting waves, an analytical expression that describes the relationship between the spatial spectra of the object $\tilde{A}_4(\kappa, m)$ and signal $\tilde{A}_{30}(\kappa)$ waves on the upper face of the nonlinear layer, considering the force of gravity acting on nanoparticles, was obtained, as follows:

$$\tilde{A}_4(\kappa,m) = -i\frac{k}{n_l}\frac{\mathrm{d}n}{\mathrm{d}T}A_{20}\exp(-iP)\sum_{j=1}^{5}G_j(\kappa,m)\times \qquad (2)$$
$$\times\frac{\exp\left\{\left[\lambda_j(\kappa,m)-\lambda_3(\kappa,m)\right]\ell\right\}-1}{\lambda_j(\kappa,m)-\lambda_3(\kappa,m)}$$

where

$$G_j(\kappa,m) = -\frac{D_{12}}{D_{22}}C_j(\kappa,m),\ j = 1,\ 2,\ 3,$$

$$G_{4,5}(\kappa,m) = \mp\frac{1}{2}\operatorname{csch}(\kappa\ell)\sum_{j=1}^{3}G_j(\kappa,m)\times$$
$$\times\left\{\exp\left[\lambda_j(\kappa,m)\ell\right]-\exp\left[\lambda_{5,4}(\kappa,m)\ell\right]\right\},$$

$$C_{1,2}(\kappa,m)\mp C_3(\kappa,m)\left(\left[\lambda_1(\kappa,m)+\lambda_2(\kappa,m)-\right.\right.$$
$$\left.\left.-\lambda_3(\kappa,m)\right]\left\{\exp\left[\lambda_{2,1}(\kappa,m)\ell\right]-\exp\left[\lambda_3(\kappa,m)\ell\right]\right\}\right)/$$
$$/\left(\lambda_{2,1}(\kappa,m)\left\{\exp\left[\lambda_2(\kappa,m)\ell\right]-\exp\left[\lambda_1(\kappa,m)\ell\right]\right\}\right),$$

$$C_3(\kappa,m) = \left(\gamma A_{10}\tilde{A}^*_{30}(\kappa)\left[\kappa^2-\lambda_3^2(\kappa,m)\right]\right)/$$
$$/\left(D_{22}\left\{\kappa^2-\lambda_3^2(\kappa,m)+\lambda_3(\kappa,m)\times\right.\right.$$
$$\left.\left.\times\left[\lambda_1(\kappa,m)+\lambda_2(\kappa,m)\right]\right\}\right),$$

$$\lambda_{1,2}(\kappa,m) = \frac{mg_z}{2k_BT_0}\left[1\pm\sqrt{1+\left(\frac{2k_BT_0}{mg_z}\kappa^2\right)^2}\right],$$

$$\lambda_3(\kappa,m) = -i\frac{\kappa^2}{2k},$$

$$\lambda_{4,5}(\kappa,m) = \pm\kappa,$$

where k is the wave number; κ is the spatial frequency of the object wave; A_{10} and A_{20} are the amplitudes of pump waves 1 and 2 on the upper and lower faces of the nonlinear layer, respectively; P is the phase shift that occurs when pump waves propagate in a nonlinear medium; D_{11} and D_{12} are the thermal conductivity and diffusion coefficients, respectively; D_{12} and γ are coefficients describing the Dufour effect and the phenomenon of electrostriction, respectively; m is the effective mass of one nanoparticle corrected for the Archimedes force; g_z is the projection of the acceleration of gravity on the Z-axis directed vertically; k_B is the Boltzmann constant; and T_0 is the temperature of the medium in the absence of radiation.

Eq. (2) was obtained using the following boundary conditions for changes in concentration and temperature:

(1) the absence of a complete flow of particles through the faces of the nonlinear layer [17; 26; 27],

(2) the constant temperature on the faces [15; 17; 18].

The analysis of Eq. (2) reveals that, for a heterogeneous monodisperse medium, provided that the signal wave is a wave from a point source located on the upper edge of the nonlinear layer $\tilde{A}_{30}(\kappa) = \text{const}$, without considering the force of gravity acting on nanoparticles, with increasing spatial frequency, the modulus of the spatial spectrum of the object wave $\tilde{A}_4(\kappa, m \to 0)$ increases and reaches a constant value at high spatial frequencies $\kappa \to 0{,}1k$ [15; 18].

The flow of nanoparticles caused by the action of gravity on them leads to the appearance of a maximum in the module of the spatial spectrum of the near-zero spatial frequency $\kappa \to 0$ [17]. In the spatial spectrum of the object wave, there is the spatial frequency $\kappa_{\min}$ at which the spatial spectrum has a value of zero, i.e., $\tilde{A}_4(\kappa_{\min}, m) = 0$.

2. Accounting for the size distribution of nanoparticles

Let us consider a four-wave interaction in a heterogeneous polydisperse medium containing spherical nanoparticles with radius a, the fraction of which varies in accordance with the distribution function $f(a)$. Then, the spatial spectrum of the object wave on the nonlinear layer upper face can be represented as a coherent "sum" of spatial spectra determined using Eq. (2), as follows:

$$\tilde{A}_4'(\kappa) = \int_{a_1}^{a_2} \tilde{A}_4(\kappa, a) f(a) da, \tag{3}$$

where a_1 and a_2 are the smallest and largest radii of nanoparticles in the medium, respectively.

The equations for the effective mass, diffusion coefficients, Dufour effect, and electrostriction can be expressed as follows [9; 24; 28]:

$$m = \frac{4}{3}\pi(\rho_p - \rho_l)a^3, \quad D_{22} = \frac{k_B T_0}{6\pi\eta a}, \tag{4}$$

$$D_{12} = \frac{3k_B T_0^3 S_T D_{22}}{4\pi C_0 a^3}, \quad \gamma = \frac{4\pi C_0 D_{22} n_l (n_p^2 - n_l^2) a^3}{c k_B T_0 (n_p^2 + 2n_l^2)},$$

where n_p and C_0 are the refractive index and concentration of nanoparticles in the absence of radiation, respectively; S_T is the Soret coefficient; η is the liquid viscosity; ρ_l and ρ_p are the densities of the liquid and particles, respectively; and c is the speed of light in vacuum.

Let us assume that the size distribution of nanoparticles is described by the following normal distribution [24; 29]:

$$f(a) = \frac{1}{\sqrt{2\pi}\sigma} \exp\left[-\frac{(a-a_0)^2}{2\sigma^2}\right], \tag{5}$$

where a_0 is the average radius of nanoparticles and σ is the mean–square deviation.

By substituting Eqs. (2), (4), and (5) into Eq. (3), we obtain the following equation for the spatial spectrum of the object wave on the upper face of the nonlinear layer, considering the size distribution of nanoparticles:

$$\tilde{A}_4'(\kappa) = -i\frac{k}{\sqrt{2\pi}\sigma n_l}\frac{dn}{dT} A_{20} \times \tag{6}$$

$$\sum_{j=1}^{5} \int_{a_1}^{a_2} G_j(\kappa, a) \frac{\exp\left\{\left[\lambda_j(\kappa, a) - \lambda_3(\kappa, a)\right]\ell\right\} - 1}{\lambda_j(\kappa, a) - \lambda_3(\kappa, a)} \times$$

$$\exp\left[-\frac{(a-a_0)^2}{2\sigma^2}\right] da.$$

When deriving Eq. (6), we assume that the phase shift caused by the propagation of pump waves in a nonlinear medium can be neglected ($P \ll \pi$).

When considering the size distribution of nanoparticles, the moduli of the spatial spectrum of the object wave near-zero $|\tilde{A}_{40}| = |\tilde{A}_4'(\kappa \to 0)|$ and at high spatial frequencies $|\tilde{A}_{4\max}| = |\tilde{A}_4'(\kappa \to 0{,}1k)|$ are determined as follows:

$$|\tilde{A}_{40}| = \left| H \int_{a_1}^{a_2} \frac{4\pi(\rho_p - \rho_l) g_z \ell a^2}{3k_B T_0} \times \right. \tag{7}$$

$$\left(\frac{1}{2} + \left\{ \exp\left[\frac{4\pi(\rho_p - \rho_l) g_z \ell a^3}{3k_B T_0} \right] - 1 \right\}^{-1} - \frac{1}{a} \right) \times$$

$$\left. \times \exp\left[-\frac{(a-a_0)^2}{2\sigma^2} \right] da \right|,$$

$$|\tilde{A}_{4\max}| = \left| H \int_{a_1}^{a_2} \left[a - i\frac{2\pi(\rho_p - \rho_l) g_z a^4}{3k k_B T_0} \right]^{-1} \times \right. \tag{8}$$

$$\left. \times \exp\left[-\frac{(a-a_0)^2}{2\sigma^2} \right] da \right|.$$

where

$$H = \frac{k k_B T_0^2 S_T A_{10} A_{20} \tilde{A}_{30}^* \ell (n_p^2 - n_l^2)}{(\sqrt{2\pi})^3 \sigma\eta c D_{11} (n_p^2 + 2n_l^2)} \frac{dn}{dT}.$$

It follows from the analysis of Eqs. (6) to (8), considering Eqs. (2) and (4) that the intensity of the pump waves, viscosity, Soret coefficient, and thermo-optical coefficient of the liquid do not affect the spatial selectivity of FRC.

3. Discussion of the results

Fig. 1 shows the normalized modules of the spatial spectra of the object wave at different average radii of nanoparticles. Normalization was performed to obtain a constant value of the module of the spatial spectrum $|\tilde{A}_{4\max}|$.

Given the size distribution of nanoparticles (in this case, the numerical integration of Eq. (3) was performed from $a_1 = 1$ nm to $a_2 = 300$ nm) does not qualitatively change the form of the modules of the

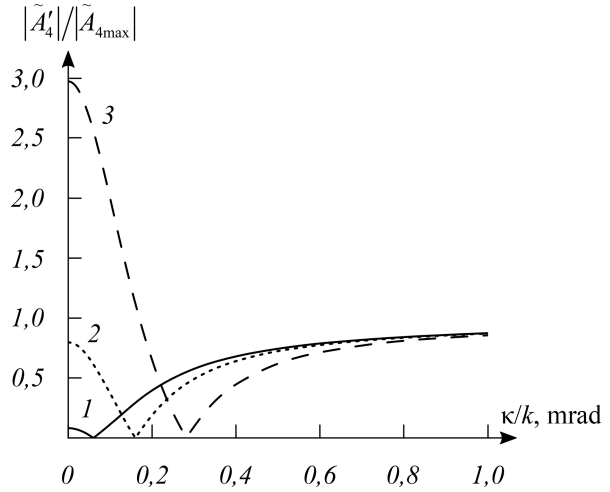

Fig. 1. Spatial spectra modules of the object wave without regarding the size dispersion of nanoparticles at $\ell = 1$ mm, $a_0 = 100$ (*1*), 150 (*2*), 200 nm (*3*)

Рис. 1. Модули пространственных спектров объектной волны без учета дисперсии наночастиц по размерам при $\ell = 1$ мм, $a_0 = 100$ (*1*), 150 (*2*) и 200 нм (*3*)

spatial spectra of the object wave. An increase in the mean–square deviation leads to a change in the values of the modules of the spatial spectrum of the object wave $|\tilde{A}_{40}|$ and $|\tilde{A}_{4\max}|$ to a shift in the spatial frequency $\kappa_{\min}$ to the region of higher values.

As in Ref. [17], we introduce the parameter ξ characterizing the ratio of the modules of the spatial spectrum of the object wave near-zero and at high spatial frequencies:

$$\xi = \frac{|\tilde{A}_{40}|}{|\tilde{A}_{4\max}|}. \qquad (9)$$

Let us use the parameter ξ to analyze the influence of the parameters of the size distribution of nanoparticles on the spatial selectivity of FRC. Let us introduce the boundary values $\xi_1 = 0{,}5$ and $\xi_2 = 2$. From the analysis of the spatial spectra of the object wave, three types of spectra, which correspond to different values of the average radius and mean–square deviation, can be distinguished.

If $\xi < \xi_1$, then the FRC filters the high spatial frequencies of the object wave by cutting out the low-frequency band (Fig. 1, curve 1), as shown, for example, in Refs. [14; 17]. Spatial selectivity can be characterized by the half-width of the spatial frequency band $\Delta\kappa$ of cutout FRCs from the spatial spectrum of the object wave, which is determined by the level $|\tilde{A}_{4\max}|/2$.

For a nonlinear medium containing nanoparticles, for which the condition $\xi_1 \le \xi \le \xi_2$ is met, the modulus of the spatial spectrum of the object wave has the form of a cutout ring with a diameter of $2\kappa_{\min}$ (Fig. 1, curve 2). In this case, the spatial selectivity of FRC can be characterized by the radius $\kappa_{\min}$ and width of the ring $\Delta\kappa_1$, determined using the following equation [16; 17]:

$$\Delta\kappa_1 = \Delta\kappa - \kappa_1, \qquad (10)$$

where the spatial frequency κ_1 is determined under the condition

$$|\tilde{A}'_4(\kappa = \kappa_1)| = |\tilde{A}_{4\max}|/2, \quad \kappa_1 < \kappa_{\min}.$$

Under the condition $\xi > \xi_2$, a pronounced maximum is recorded in the spatial spectrum of the object wave near-zero spatial frequency (Fig. 1, curve 3). Spatial selectivity in this case can be characterized by the half-width of the maximum, determined by the level $|\tilde{A}_{40}|/2$.

The analysis of Eq. (3) shows that, for a fixed thickness of the nonlinear medium, the shape of the spatial spectrum of the object wave is mainly determined by the average radius of the nanoparticles. Therefore, we refer to spatial spectra with $\xi < \xi_1$, $\xi_1 \le \xi \le \xi_2$, and $\xi > \xi_2$ as the spectra corresponding to the small, intermediate, and large average radii of nanoparticles. Thus, the modules of the spatial spectra of the object wave shown in Fig. 1 correspond to the small (Curve 1), intermediate (Curve 2), and large (Curve 3) average radii of nanoparticles.

Fig. 2 shows that, for different thicknesses of the nonlinear medium, the parameter ranges in the size distribution of nanoparticles correspond to the small, intermediate, and large average radii of nanoparticles. An increase in the layer thickness leads to a shift in the boundary values ξ_1 and ξ_2 to the region of smaller average radii of nanoparticles. At $l \ge 1$ mm, a change in the mean–square deviation in the size distribution of nanoparticles within $0 \le \sigma \le 40$ nm has only a slight effect on the boundary value ξ_2.

The analysis of Eq. (2) reveals that, for a heterogeneous monodisperse medium, the ratio of the moduli of the spatial spectra of the object wave near-zero and at high spatial frequencies depends not only on the mass of one nanoparticle but also on the layer thickness, which can be expressed as follows:

$$\xi(m,\ell) = \sqrt{1+\left(\frac{mg_z}{2kk_BT_0}\right)^2} \times \qquad (11)$$

$$\times \left| \frac{mg_z\ell}{k_BT_0}\left\{\frac{1}{2} + \left[\exp\left(\frac{mg_z\ell}{k_BT_0}\right) - 1\right]^{-1}\right\} - 1 \right|.$$

For a fixed size of nanoparticles, an increase in the thickness of the heterogeneous medium leads to an increase in the parameter ξ and, consequently,

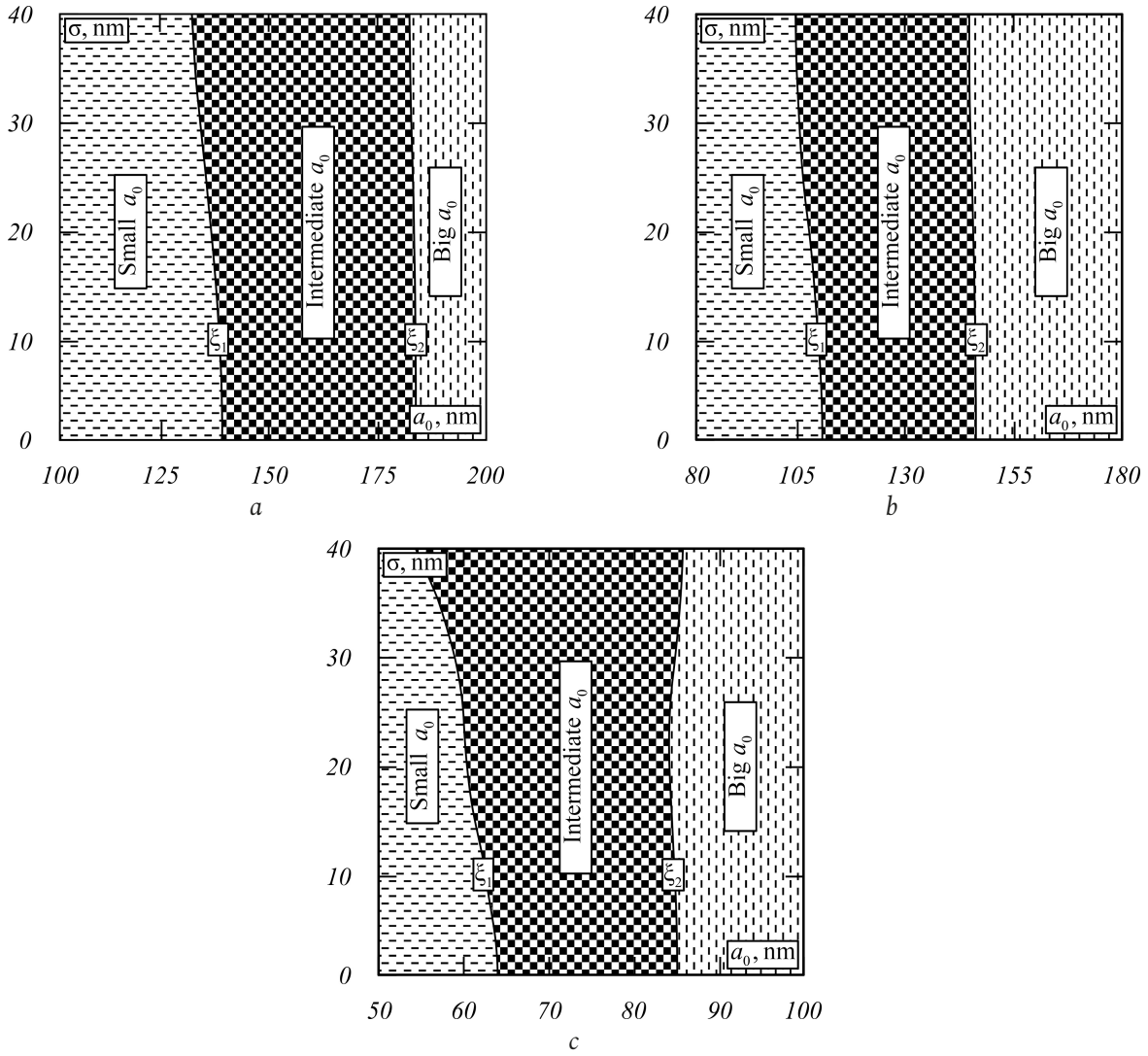

Fig. 2. Areas of average radii of nanoparticles depending on their average radius and standard deviation at $\ell = 1$ (*a*), 2 (*b*) и 10 mm (*c*)
Рис. 2. Области средних радиусов наночастиц в зависимости от их среднего радиуса и среднеквадратичного отклонения при $\ell = 1$ (*а*), 2 (*б*) и 10 мм (*в*)

to a decrease in the size of nanoparticles, at which this parameter reaches boundary values. This finding explains the shift in the boundary values ξ_1 and ξ_2 (Fig. 2) to the region of smaller average radii of nanoparticles with the increase in the thickness of the nonlinear layer.

Fig. 3 shows the dependence of the half-width of the cutout spatial frequency bands on the mean–square deviation at various average radii of nanoparticles. With an increase in both the average radius and the mean–square deviation, an increase in the half-width of the cutout spatial frequency bands is noted.

Fig. 4 shows the dependence of the width of the cutout ring on the mean–square deviation of nanoparticles corresponding to the intermediate average radii. In terms of the dependence of $\Delta\kappa_1$ on σ, a minimum value, which shifts to the region of smaller mean–square deviation values with the increase in the average radius of nanoparticles, is recorded. Notably, for any fixed value of $\sigma \le 35$ nm, the value of $\Delta\kappa_1$ monotonically decreases with the increase in a_0, which is also observed in the case of a heterogeneous monodisperse medium ($\sigma \to 0$) [17].

For nanoparticles with an average radius in the range of large radii, the half-width of the maximum near-zero spatial frequency increases with the increase in the average radius of the nanoparticles, and at $\sigma \le 40$ nm, it does not depend on the mean–square deviation.

Here, we present estimates of the influence of the size distribution of nanoparticles on the spatial selectivity of FRC at a thickness of 1 mm in a heterogeneous polydisperse nonlinear medium.

In the region of parameters corresponding to small average radii of nanoparticles, with a mean–square deviation of 40 nm compared with a monodisperse

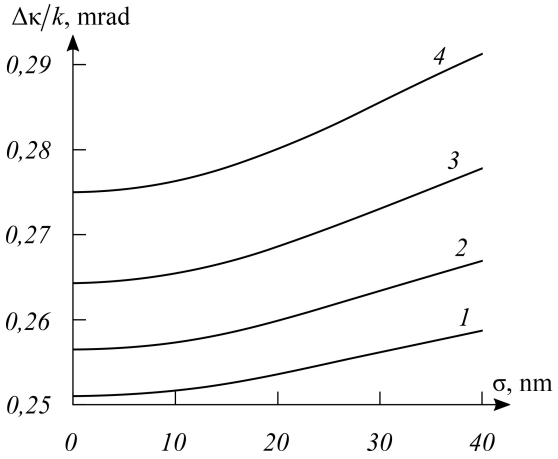

Fig. 3. Graph of the dependence of the half-width of the cut spatial frequency band on the standard deviation at $\ell = 1$ mm, $a_0 = 100$ (*1*), 110 (*2*), 120 (*3*), 130 nm (*4*)
Рис. 3. График зависимости полуширины полосы вырезанных пространственных частот от среднеквадратичного отклонения при $\ell = 1$ мм, $a_0 = 100$ (*1*), 110 (*2*), 120 (*3*), 130 нм (*4*)

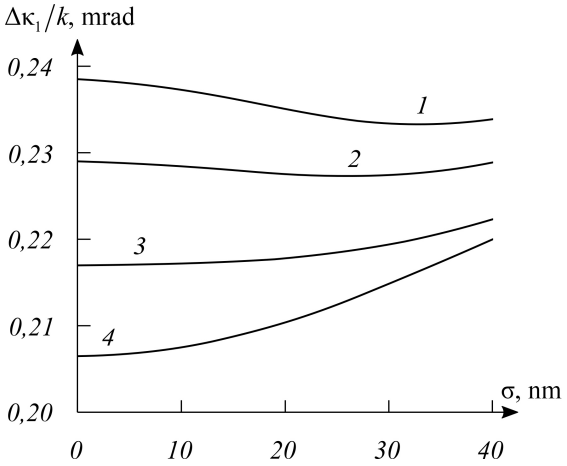

Fig. 4. Graph of the dependence of the cut "ring" width on the standard deviation at $\ell = 1$ mm, $a_0 = 144$ (*1*), 148 (*2*), 156 (*3*), 190 nm (*4*)
Рис. 4. График зависимости ширины вырезанного «кольца» от среднеквадратичного отклонения при $\ell = 1$ мм, $a_0 = 144$ (*1*), 148 (*2*), 156 (*3*), 190 нм (*4*)

nonlinear medium, the half-width of the cutout spatial frequency band for a_0 of 100 and 130 nm increases by 3,1 % and 6,0 %, respectively.

In the region of parameters corresponding to intermediate average radii of nanoparticles, at the same σ value of 40 nm, compared with a monodisperse nonlinear medium, the width of the cutout ring at a_0 of 180 nm increases by 6,0 % and at a_0 of 144 nm decreases by 1,9 %. In this case, the radius of the ring increases by 7,3 % and 12,7 %.

Notably, without considering the flow of nanoparticles caused by the action of gravity on them, the spatial selectivity of FRC in a heterogeneous polydisperse medium ceases to depend on the mean–square deviation in the size distribution of nanoparticles; only the FRC reflection coefficient changes [24].

Conclusion

The dependence of the parameters characterizing the spatial selectivity of FRC in a transparent polydisperse heterogeneous medium, considering the flow of nanoparticles caused by the action of gravity on them, on the mean–square deviation and average radius of nanoparticles was analyzed.

If, in the range of small average radii of nanoparticles, the half-width of the spatial frequency, cut out from the module of the spatial spectrum of the object wave, increases with the increase in the mean–square deviation, then, in the range of intermediate average radii of nanoparticles, where the module of the spatial spectrum of the object wave has the form of a cutout ring, an increase in the mean–square deviation can lead, depending on the average radius of nanoparticles, to an increase or a decrease in the width of the ring.

At large average radii of nanoparticles, the mean–square deviation in the size distribution of nanoparticles does not affect the half-width of the maximum of the spatial spectrum of the object wave near-zero spatial frequency.

References

1. Liu X. et al. Nonlinear four-wave mixing with enhanced diversity and selectivity via spin and orbital angular momentum conservation. *APL Photonics*, 2020, vol. 5, p. 010802. DOI: https://doi.org/10.1063/1.5130715
2. Paesani S. et al. Near-ideal spontaneous photon sources in silicon quantum photonics. *Nature Communications*, 2020, vol. 11, p. 2505. DOI: https://doi.org/10.1038/s41467-020-16187-8
3. Pandya N. et al. Creation of the maximum coherence via adiabatic passage in the four-wave mixing process of coherent anti-stokes Raman scattering. *Chemical Physics Letters*, 2020, vol. 738, p. 136763. DOI: https://doi.org/10.1016/j.cplett.2019.136763
4. Giannakopoulou N. et al. Four-wave-mixing microscopy reveals non-colocalisation between gold nanoparticles and fluorophore conjugates inside cells. *Nanoscale*, 2020, vol. 12, pp. 4622–4635. DOI: https://doi.org/10.1039/c9nr08512b
5. Erokhon A.I. et al. Stimulated thermal scattering in two-photon absorbing nanocolloids under laser radiation of nanosecond-to-picosecond pulse widths. *Nanomaterials*, 2022, vol. 12, p. 2567, DOI: https://doi.org/10.3390/nano12152567
6. Borri P. et al. Imaging and tracking single plasmonic nanoparticles in 3D background-free with four-wave mixing interferometry. *Proceedings of SPIE*, 2019, vol. 10894, p. 108940Z. DOI: https://doi.org/10.1117/12.2507618

7. Geng Y. et al. Silver nanoparticle-enhanced four-wave mixing (FWM) imaging technique for visualizing sialic acid on cell membrane. *Sensors and Actuators B. Chemical*, 2019, vol. 301, p. 127074. DOI: https://doi.org/10.1016/j.snb.2019.127074

8. Vorob'eva E.V. et al. Point smearing function of a four-wave radiation converter in a multimode waveguide with Kerr nonlinearity. *Physics of Wave Processes and Radio Systems*, 2021, vol. 24, no. 1, pp. 15–21. DOI: https://doi.org/10.18469/1810-3189.2021.24.1.15-21 (In Russ.)

9. Ivanov V.I., Ivanova G.D. Non-resonance mechanisms of optical nonlinearities of aerosols. *Proceedings of SPIE*, 2018, vol. 10833, p. 108331S. DOI: https://doi.org/10.1117/12.2504378

10. Moreels I. et al. Spectroscopy of the nonlinear refractive index of colloidal PbSe nanocrystals. *Applied Physics Letters*, 2006, vol. 89, p. 193106. DOI: https://doi.org/10.1063/1.2385658

11. Arandian A., Karimzadeh R., Faizabadi S.Y. The effect of laser wavelength and concentration on thermal nonlinear refractive index of grapheme suspensions. *Nano*, 2015, vol. 10, no. 4, p. 1550053. DOI: https://doi.org/10.1142/S1793292015500538

12. Cherepanov I.N. On the redistribution of impurities in colloidal mixtures. *Zhurnal tekhnicheskoy fiziki*, 2018, vol. 88, no. 12, pp. 1763–1770. DOI: https://doi.org/10.21883/JTF.2018.12.46775.2589 (In Russ.)

13. Voyutskiy S.S. *Colloid Chemistry Course*. Moscow: Khimiya, 1975, 512 p. (In Russ.)

14. Ivakhnik V.V., Savel'ev M.V. Non-stationary four-wave interaction in a transparent two-component medium. *Komp'yuternaya optika*, 2018, vol. 42, no. 2, pp. 227–235. DOI: https://doi.org/10.18287/2412-6179-2018-42-2-227-235 (In Russ.)

15. Ivakhnik V.V., Savel'ev M.V. Degenerate four-wave mixing in transparent two-component medium considering spatial structure of the pump waves. *Journal of Physics. Conference Series*, 2016, vol. 737, pp. 012007. DOI: https://doi.org/10.1088/1742-6596/737/1/012007

16. Ivakhnik V.V., Savel'ev M.V. Spatial selectivity of a four-wave radiation converter in an absorbing two-component medium at high reflection coefficients. *Physics of Wave Processes and Radio Systems*, 2018, vol. 21, no. 2, pp. 5–13. URL: https://journals.ssau.ru/pwp/article/view/7029/6888 (In Russ.)

17. Savel'ev M.V., Ivakhnik V.V. Spatial selectivity of a four-wave radiation converter taking into account the force of gravity acting on nanoparticles dissolved in a transparent liquid. *Izvestiya vysshikh uchebnykh zavedeniy. Radiofizika*, 2020, vol. 63, no. 8, pp. 694–703. URL: https://elibrary.ru/item.asp?id=44851030 (In Russ.)

18. Remzov A.D., Savel'ev M.V. Counter four-wave interaction in a transparent suspension of nanoparticles in the Earth's gravity field. *Izvestiya Rossiyskoy akademii nauk. Seriya fizicheskaya*, 2021, vol. 85, no. 12, pp. 1770–1775. DOI: https://doi.org/10.31857/S0367676521120267 (In Russ.)

19. Ivakhnik V.V., Savel'ev M.V. Spatial selectivity of a four-wave radiation converter taking into account the thermal diffusion and electrostrictive mechanisms of nonlinearity. *Physics of Wave Processes and Radio Systems*, 2013, vol. 16, no. 1, pp. 6–11. URL: https://elibrary.ru/item.asp?id=20211855 (In Russ.)

20. Ershov A.E. et al. Optodynamic phenomena in aggregates of polydisperse plasmonic nanoparticles. *Applied Physics B*, 2014, vol. 115, pp. 547–560. DOI: https://doi.org/10.1007/s00340-013-5636-6

21. Zoriniants G. et al. Background-free 3D nanometric localization and sub-nm asymmetry detection of single plasmonic nanoparticles by four-wave mixing interferometry with optical vortices. *Physical Review X*, 2017, vol. 7, pp. 041022. DOI: https://doi.org/10.1103/PhysRevX.7.041022

22. Uchida K. et al. Optical nonlinearities of a high concentration of small metal particles dispersed in glass: copper and silver particles. *Journal of the Optical Society of America B*, 1994, vol. 11, no. 7, pp. 1236–1243. DOI: https://doi.org/10.1364/JOSAB.11.001236

23. Bloemer M.J., Haus J.W., Ashley P.R. Degenerate four-wave mixing in colloidal gold as a function of particle size. *Journal of the Optical Society of America B*, 1990, vol. 7, no. 5, pp. 790–795. DOI: https://doi.org/10.1364/JOSAB.7.000790

24. Al'debeneva K.N., Ivakhnik V.V., Savel'ev M.V. Effect of particle size distribution on the characteristics of a four-wave radiation converter in a transparent two-component medium. *Physics of Wave Processes and Radio Systems*, 2019, vol. 22, no. 1, pp. 4–9. DOI: https://doi.org/10.18469/1810-3189.2019.22.1.4-9 (In Russ.)

25. Gerakis A. et al. Four-wave-mixing approach to in situ detection of nanoparticles. *Physical Review Applied*, 2018, vol. 9, p. 014031. DOI: https://doi.org/10.1103/PhysRevApplied.9.014031

26. Larsson C., Kumar S. Nonuniformities in miscible two-layer two-component thin liquid films. *Physical Review Fluids*, 2021, vol. 6, p. 034004. DOI: https://doi.org/10.1103/PhysRevFluids.6.034003

27. Khe V.K. et al. Sedimentation of particles by the light pressure in nanosuspension. *Proceedings of SPIE*, 2017, vol. 10466, p. 104664K. DOI: https://doi.org/10.1117/12.2288774

28. Behera S.K. et al. Effects of polydispersity on the glass transition dynamics of aqueous suspensions of soft spherical colloidal particles. *Physical Review Materials*, 2017, vol. 1, p. 055603. DOI: https://doi.org/10.1103/PhysRevMaterials.1.055603

29. Ivanov V.I., Pyachin S.A. Separation of particles in a polydisperse nanosuspension in the field of laser radiation. *Fiziko-khimicheskie aspekty izucheniya klasterov, nanostruktur i nanomaterialov*, 2021, no. 13, pp. 146–155. DOI: https://doi.org/10.26456/pcascnn/2021.13.146 (In Russ.)

Список литературы

1. Nonlinear four-wave mixing with enhanced diversity and selectivity via spin and orbital angular momentum conservation / X. Liu [et al.] // APL Photonics. 2020. Vol. 5. P. 010802. DOI: https://doi.org/10.1063/1.5130715

2. Near-ideal spontaneous photon sources in silicon quantum photonics / S. Paesani [et al.] // Nature Communications. 2020. Vol. 11. P. 2505. DOI: https://doi.org/10.1038/s41467-020-16187-8

3. Creation of the maximum coherence via adiabatic passage in the four-wave mixing process of coherent anti-Stokes Raman scattering / N. Pandya [et al.] // Chemical Physics Letters. 2020. Vol. 738. P. 136763. DOI: https://doi.org/10.1016/j.cplett.2019.136763

4. Four-wave-mixing microscopy reveals non-colocalisation between gold nanoparticles and fluorophore conjugates inside cells / N. Giannakopoulou [et al.] // Nanoscale. 2020. Vol. 12. P. 4622–4635. DOI: https://doi.org/10.1039/c9nr08512b

5. Stimulated thermal scattering in two-photon absorbing nanocolloids under laser radiation of nanosecond-to-picosecond pulse widths / A.I. Erokhon [et al.] // Nanomaterials. 2022. Vol. 12. P. 2567. DOI: https://doi.org/10.3390/nano12152567

6. Imaging and tracking single plasmonic nanoparticles in 3D background-free with four-wave mixing interferometry / P. Borri [et al.] // Proceedings of SPIE. 2019. Vol. 10894. P. 108940Z. DOI: https://doi.org/10.1117/12.2507618

7. Silver nanoparticle-enhanced four-wave mixing (FWM) imaging technique for visualizing sialic acid on cell membrane / Y. Geng [et al.] // Sensors and Actuators B. Chemical. 2019. Vol. 301. P. 127074. DOI: https://doi.org/10.1016/j.snb.2019.127074

8. Функция размытия точки четырехволнового преобразователя излучения в многомодовом волноводе с керровской нелинейностью / Е.В. Воробьева [и др.] // Физика волновых процессов и радиотехнические системы. 2021. Т. 24, № 1. С. 15–21. DOI: https://doi.org/10.18469/1810-3189.2021.24.1.15-21

9. Ivanov V.I., Ivanova G.D. Non-resonance mechanisms of optical nonlinearities of aerosols // Proceedings of SPIE. 2018. Vol. 10833. P. 108331S. DOI: https://doi.org/10.1117/12.2504378

10. Spectroscopy of the nonlinear refractive index of colloidal PbSe nanocrystals / I. Moreels [et al.] // Applied Physics Letters. 2006. Vol. 89. P. 193106. DOI: https://doi.org/10.1063/1.2385658

11. Arandian A., Karimzadeh R., Faizabadi S.Y. The effect of laser wavelength and concentration on thermal nonlinear refractive index of grapheme suspensions // Nano. 2015. Vol. 10, no. 4. P. 1550053. DOI: https://doi.org/10.1142/S1793292015500538

12. Черепанов И.Н. О перераспределении примеси в коллоидных смесях // Журнал технической физики. 2018. Т. 88, № 12. С. 1763–1770. DOI: https://doi.org/10.21883/JTF.2018.12.46775.2589

13. Воюцкий С.С. Курс коллоидной химии. М.: Химия, 1975. 512 с.

14. Ивахник В.В., Савельев М.В. Нестационарное четырехволновое взаимодействие в прозрачной двухкомпонентной среде // Компьютерная оптика. 2018. Т. 42, № 2. С. 227–235. DOI: https://doi.org/10.18287/2412-6179-2018-42-2-227-235

15. Ivakhnik V.V. Savel'ev M.V. Degenerate four-wave mixing in transparent two-component medium considering spatial structure of the pump waves // Journal of Physics. Conference Series. 2016. Vol. 737. P. 012007. DOI: https://doi.org/10.1088/1742-6596/737/1/012007

16. Ивахник В.В., Савельев М.В. Пространственная селективность четырехволнового преобразователя излучения в поглощающей двухкомпонентной среде при больших коэффициентах отражения // Физика волновых процессов и радиотехнические системы. 2018. Т. 21, № 2. С. 5–13. URL: https://journals.ssau.ru/pwp/article/view/7029/6888

17. Савельев М.В., Ивахник В.В. Пространственная селективность четырехволнового преобразователя излучения с учетом силы тяжести, действующей на растворенные в прозрачной жидкости наночастицы // Известия высших учебных заведений. Радиофизика. 2020. Т. 63, № 8. С. 694–703. URL: https://elibrary.ru/item.asp?id=44851030

18. Ремзов А.Д., Савельев М.В. Встречное четырехволновое взаимодействие в прозрачной суспензии наночастиц в поле тяжести Земли // Известия Российской академии наук. Серия физическая. 2021. Т. 85, № 12. С. 1770–1775. DOI: https://doi.org/10.31857/S0367676521120267

19. Ивахник В.В., Савельев М.В. Пространственная селективность четырехволнового преобразователя излучения с учетом термодиффузионного и электрострикционного механизмов нелинейности // Физика волновых процессов и радиотехнические системы. 2013. Т. 16, № 1. С. 6–11. URL: https://elibrary.ru/item.asp?id=20211855

20. Optodynamic phenomena in aggregates of polydisperse plasmonic nanoparticles / A.E. Ershov [et al.] // Applied Physics B. 2014. Vol. 115. P. 547–560. DOI: https://doi.org/10.1007/s00340-013-5636-6

21. Background-free 3D nanometric localization and sub-nm asymmetry detection of single plasmonic nanoparticles by four-wave mixing interferometry with optical vortices / G. Zoriniants [et al.] // Physical Review X. 2017. Vol. 7. P. 041022. DOI: https://doi.org/10.1103/PhysRevX.7.041022

22. Optical nonlinearities of a high concentration of small metal particles dispersed in glass: copper and silver particles / K. Uchida [et al.] // Journal of the Optical Society of America B. 1994. Vol. 11, no. 7. P. 1236–1243. DOI: https://doi.org/10.1364/JOSAB.11.001236

23. Bloemer M.J., Haus J.W., Ashley P.R. Degenerate four-wave mixing in colloidal gold as a function of particle size // Journal of the Optical Society of America B. 1990. Vol. 7, no. 5. P. 790–795. DOI: https://doi.org/10.1364/JOSAB.7.000790

24. Альдебенева К.Н., Ивахник В.В., Савельев М.В. Влияние распределения частиц по размерам на характеристики четырехволнового преобразователя излучения в прозрачной двухкомпонентной среде // Физика волновых процессов и радиотехнические системы. 2019. Т. 22, № 1. С. 4–9. DOI: https://doi.org/10.18469/1810-3189.2019.22.1.4-9

25. Four-wave-mixing approach to in situ detection of nanoparticles / A. Gerakis [et al.] // Physical Review Applied. 2018. Vol. 9. P. 014031. DOI: https://doi.org/10.1103/PhysRevApplied.9.014031

26. Larsson C., Kumar S. Nonuniformities in miscible two-layer two-component thin liquid films // Physical Review Fluids. 2021. Vol. 6. P. 034004. DOI: https://doi.org/10.1103/PhysRevFluids.6.034003

27. Sedimentation of particles by the light pressure in nanosuspension / V.K. Khe [et al.] // Proceedings of SPIE. 2017. Vol. 10466. P. 104664K. DOI: https://doi.org/10.1117/12.2288774

28. Effects of polydispersity on the glass transition dynamics of aqueous suspensions of soft spherical colloidal particles / S.K. Behera [et al.] // Physical Review Materials. 2017. Vol. 1. P. 055603. DOI: https://doi.org/10.1103/PhysRevMaterials.1.055603

29. Иванов В.И., Пячин С.А. Сепарация частиц в полидисперсной наносуспензии в поле лазерного излучения // Физико-химические аспекты изучения кластеров, наноструктур и наноматериалов. 2021. Вып. 13. С. 146–155. DOI: https://doi.org/10.26456/pcascnn/2021.13.146

Физика волновых процессов и радиотехнические системы
2023. Т. 26, № 1. С. 9–17

DOI 10.18469/1810-3189.2023.26.1.9-17
УДК 535.317.1

Дата поступления 24 ноября 2022
Дата принятия 26 декабря 2022

Влияние дисперсности наночастиц в прозрачной жидкости на пространственные характеристики четырехволнового преобразователя излучения

В.В. Ивахник, М.В. Савельев

Самарский национальный исследовательский университет имени академика С.П. Королева
443086, Российская Федерация, г. Самара,
Московское шоссе, 34

Аннотация – В работе исследованы пространственные характеристики четырехволнового преобразователя излучения в прозрачной гетерогенной полидисперсной среде с учетом потока наночастиц, обусловленного действием силы тяжести, при нормальном распределением частиц по размерам. Выделено три диапазона средних радиусов наночастиц (малые, промежуточные и большие), для которых характерны различные виды пространственных спектров объектной волны. Показано, что в диапазоне малых средних радиусов наночастиц рост среднеквадратичного отклонения приводит к увеличению полуширины полосы пространственных частот, вырезаемых четырехволновым преобразователем излучения из пространственного спектра объектной волны. В диапазоне промежуточных средних радиусов наночастиц рост среднеквадратичного отклонения может приводить как к увеличению, так и к уменьшению ширины вырезаемого четырехволновым преобразователем «кольца». При больших средних радиусах наночастиц изменение среднеквадратичного отклонения не влияет на пространственную селективность четырехволнового преобразователя излучения.

Ключевые слова – четырехволновой преобразователь излучения; прозрачная среда; нормальное распределение.

Information about the Authors

Valery V. Ivakhnik, Doctor of Physical and Mathematical Sciences, head of the Department of Optics and Spectroscopy, Samara National Research University, Samara, Russia.
Research interests: nonlinear optics, dynamic holography.
E-mail: ivakhnik@ssau.ru

Maxim V. Savelyev, Candidate of Physical and Mathematical Sciences, associate professor of the Department of Optics and Spectroscopy, Samara National Research University, Samara, Russia.
Research interests: nonlinear optics, dynamic holography.
E-mail: belchonokenot@mail.ru
ORCID: https://orcid.org/0000-0002-7548-0331

Информация об авторах

Ивахник Валерий Владимирович, доктор физико-математических наук, профессор, заведующий кафедрой оптики и спектроскопии Самарского национального исследовательского университета имени академика С.П. Королева, г. Самара, Россия.
Область научных интересов: нелинейная оптика, динамическая голография.
E-mail: ivakhnik@ssau.ru

Савельев Максим Валерьевич, кандидат физико-математических наук, доцент кафедры оптики и спектроскопии Самарского национального исследовательского университета имени академика С.П. Королева, г. Самара, Россия.
Область научных интересов: нелинейная оптика, динамическая голография.
E-mail: belchonokenot@mail.ru
ORCID: https://orcid.org/0000-0002-7548-0331